



**HAL**  
open science

# Massive MIMO channel estimation taking into account spherical waves

Luc Le Magoarou, Antoine Le Calvez, Stéphane Paquelet

► **To cite this version:**

Luc Le Magoarou, Antoine Le Calvez, Stéphane Paquelet. Massive MIMO channel estimation taking into account spherical waves. 2018. hal-01920442v2

**HAL Id: hal-01920442**

**<https://hal.science/hal-01920442v2>**

Preprint submitted on 8 Feb 2019

**HAL** is a multi-disciplinary open access archive for the deposit and dissemination of scientific research documents, whether they are published or not. The documents may come from teaching and research institutions in France or abroad, or from public or private research centers.

L'archive ouverte pluridisciplinaire **HAL**, est destinée au dépôt et à la diffusion de documents scientifiques de niveau recherche, publiés ou non, émanant des établissements d'enseignement et de recherche français ou étrangers, des laboratoires publics ou privés.

# Massive MIMO Channel Estimation taking into account spherical waves

Luc Le Magoarou, Antoine Le Calvez, Stéphane Paquelet  
*b<>com, Rennes, France*

**Abstract**—Massive multiple-input multiple-output (MIMO) systems are key technological components of fifth generation (5G) wireless communication systems. In such a context, geometric considerations show that the largely adopted plane wave model (PWM) of the channel potentially loses its validity. An alternative is to consider the more accurate but more complex spherical wave model (SWM). This paper introduces an intermediate parabolic wave model (ParWM), more accurate than the PWM while less complex than the SWM. The validity domains of those three physical models are assessed and estimation algorithms for the SWM and ParWM are proposed, showing a promising performance complexity trade-off.

**Index Terms**—MIMO, physical models, channel estimation.

## I. INTRODUCTION

Massive multiple-input multiple-output (massive MIMO) is an essential technology for future fifth generation (5G) wireless communication systems [1]–[4]. Using several antennas allows to exploit the spatial dimension to achieve high capacity, reliability, and energy efficiency. The term “massive” refers to systems with up to hundreds of antennas with much better performance. A typical application is in cellular networks with a base station composed of many antennas and user terminals with few antennas, commonly referred to as multi-user MIMO (MU-MIMO). Massive MIMO antenna arrays are large with respect to the wavelength, so that the compactness of the system becomes a challenge. Millimeter wave (mmWave) [5], [6] operating bands mitigate this issue by reducing the wavelength.

The MIMO channel, assumed static and considered at a single subcarrier with  $N_t$  transmit antennas and  $N_r$  receive antennas, is usually represented in the frequency domain by the channel matrix  $\mathbf{H} \in \mathbb{C}^{N_r \times N_t}$  containing the complex gains linking all the transmit/receive antenna couples. Knowledge of this matrix is required both at the transmitter and receiver to achieve the tremendous MIMO capacity [7]. Estimating the entries of  $\mathbf{H}$  amounts to determine  $N_r N_t$  complex coefficients, which is not suitable in massive MIMO systems for which this number may be very high. It is thus convenient to consider a parametric channel estimation [8]: injecting a priori information about the channel (combining antenna array geometry and propagation properties) allows to reduce the estimation complexity.

Traditionally the transmitter and receiver are assumed to

be separated by a large distance with respect to their antenna array size (greater than the Fraunhofer distance [9]), so that the spherical wavefronts are well approximated by planes. This simplifying hypothesis is known as the plane wave assumption, the corresponding physical model being referred to as the plane wave model (PWM). For massive MIMO systems involving up to several hundreds of antennas, i.e. much larger arrays, this model is not always valid and the curvature of the wavefronts cannot be neglected. In such situations, more complex but more accurate models such as the spherical wave model (SWM) might be required.

**Contributions.** In this paper, three physical parametric channel models applicable to any type of antenna array are presented. The well-known PWM and SWM are first recalled and an intermediate parabolic wave model (ParWM) is introduced, that is more accurate than the PWM while less complex than the SWM. The second contribution consists in studying the validity domains of the three models using a relative squared error metric more relevant to channel estimation than the classically used phase-shift metric. The final contribution is to propose computationally efficient channel estimation algorithms taking into account ParWM and SWM and compare them to classical algorithms assuming the PWM in a multi-user MIMO scenario.

**Related work.** The PWM validity issue as well as the need for the SWM to describe massive MIMO channels have already been studied in the literature [10]–[16]. So far, the studies are particularized either to linear and/or planar arrays, which yields less general and more complex analytical expressions and interpretations. In this paper the PWM and SWM analytical expressions are given adopting the generalization to any antenna array [8], and a new physical model is proposed: the ParWM. Different metrics are studied in the state of the art highlighting the PWM limits and the SWM benefits: in [10], [14] the authors investigate the correlation in single-user MIMO (SU-MIMO) and in MU-MIMO scenarios; in [10]–[12], [15], [16] the channel capacity issue is tackled; in [9], [13] the phase-shift difference induced by the SWM is used to define the near/far field boundary of large antenna arrays. Here the models validity domains are characterized through a relative squared error metric quantifying the overall error on the channel matrix: it is discussed and compared to phase-shift considerations as presented in [9], [13]. Finally, channel estimation algorithms taking into account the curvature of the wavefronts are proposed here for the first time, to the best of the authors’ knowledge.

This work has been performed in the framework of the Horizon 2020 project ONE5G (ICT-760809) receiving funds from the European Union. The authors would like to acknowledge the contributions of their colleagues in the project, although the views expressed in this contribution are those of the authors and do not necessarily represent the project.

## II. PROBLEM FORMULATION

**Notations.** Matrices and vectors are denoted by bold upper-case and lower-case letters:  $\mathbf{A}$  and  $\mathbf{a}$  (except 3D "spatial" vectors that are denoted  $\vec{a}$ ); its entry at the  $i$ th line and  $j$ th column by:  $a_{ij}$ .  $\mathbf{A}^T$  and  $\mathbf{A}^*$  denote a matrix transpose and conjugate, respectively. The vectorization operator and the identity matrix are denoted by  $\text{vec}(\cdot)$  and  $\mathbf{Id}$  respectively.  $\langle \cdot, \cdot \rangle$ ,  $\|\cdot\|_2$  and  $\|\cdot\|_F$  denote the Hermitian inner product, the L2-norm and the Frobenius norm.

**Geometric channel model.** Let us use the channel model of [8], in which the transmit (receive) antenna array is described by the positions of its antennas denoted  $\vec{a}_{t,j}$ ,  $j = 1, \dots, N_t$  ( $\vec{a}_{r,i}$ ,  $i = 1, \dots, N_r$ ) with respect to its centroid  $O_t$  ( $O_r$ ). Note that the coordinate systems used at the transmitter and receiver are in general different. This description is very general: it is applicable to any type of antenna array, not only to ULA and UPA as mostly found in the literature.

Each propagation path is described in the frequency domain by a complex gain  $\rho e^{j\phi}$  expressing the channel between the centroids  $O_t$  and  $O_r$ , a direction of departure (DoD)  $\vec{u}_t$  (expressed in the transmitter coordinate system) and a direction of arrival  $\vec{u}_r$  (expressed in the receiver coordinate system). Denoting  $D$  the distance between the two centroids  $O_t$  and  $O_r$  and  $D_{ij}$  is the distance between the  $j$ -th transmit antenna and the  $i$ -th receive antenna, the channel for this antenna couple is classically expressed [10]–[16] as

$$h_{ij} = \rho e^{j\phi} e^{-j\frac{2\pi}{\lambda}(D_{ij}-D)}, \quad (1)$$

where  $\lambda$  is the wavelength and the quantity  $\frac{2\pi}{\lambda}(D_{ij}-D)$  is the phase shift with respect to the reference points located at  $O_t$  and  $O_r$ . It has an important impact since it involves a division of the lengths difference  $D_{ij}-D$  by the wavelength  $\lambda$  which can be very small (1cm at 30GHz). Note that an amplitude fluctuation term also exists but is reasonably neglected since the ratio  $\frac{D}{D_{ij}}$  is very close to one in practice, because the antenna arrays are in general much smaller than the propagation distance.

**Spherical Wave Model.** Using the SWM consists in computing  $\Delta_{\text{SWM},ij} \triangleq D_{ij}-D$  using the channel parameters. In a single path LoS scenario, geometric considerations using the transmit coordinate system lead to

$$\begin{aligned} \Delta_{\text{SWM},ij} &= \|\vec{a}_{t,j} + D\vec{u}_t + \mathbf{R}(\delta)\vec{a}_{r,i}\|_2 - D \\ &= D \left( \sqrt{1 + \frac{2(\vec{a}_{r,i}\vec{u}_r - \vec{a}_{t,j}\vec{u}_t)}{D} + \frac{\|\mathbf{R}(\delta)\vec{a}_{r,i} - \vec{a}_{t,j}\|_2^2}{D^2}} - 1 \right), \end{aligned} \quad (2)$$

where  $-\vec{a}_{t,j}$  is the vector from the  $j$ -th transmit antenna to  $O_t$ ,  $D\vec{u}_t$  is the vector from  $O_t$  to  $O_r$  and  $\mathbf{R}(\delta)\vec{a}_{r,i}$  is the vector from  $O_r$  to the  $i$ -th receive antenna expressed in the transmit coordinate system ( $\mathbf{R}(\delta)$  is the rotation matrix mapping the receiver coordinate system to the transmit one which, given  $\vec{u}_t$  and  $\vec{u}_r$ , depends only on a real parameter  $\delta$  quantifying the rotation around the axis  $O_tO_r$ ). The DoD and DoA being physically the same in a LoS scenario,  $\mathbf{R}(\delta)\vec{u}_r = \vec{u}_t$ , which allows to obtain the second line of the equation. Note that in a single-antenna receiver case (i.e.  $N_r = 1$  and  $\vec{a}_{r,1} = \vec{0}$ )

which is considered hereafter,  $\mathbf{R}(\delta)$  can be omitted. Injecting (2) in (1) yields the spherical channel coefficient

$$h_{\text{SWM},ij} = \rho e^{j\phi} e^{-j2\pi\frac{D}{\lambda} \left( \sqrt{1 + \frac{2(\vec{a}_{r,i}\vec{u}_r - \vec{a}_{t,j}\vec{u}_t)}{D} + \frac{\|\mathbf{R}(\delta)\vec{a}_{r,i} - \vec{a}_{t,j}\|_2^2}{D^2}} - 1 \right)}.$$

Therefore the channel matrix  $\mathbf{H}_{\text{SWM}}$  is a deterministic function of a set of eight parameters denoted  $\boldsymbol{\theta} \triangleq \{(\rho, \phi, \vec{u}_t, \vec{u}_r, D, \delta)\}$  (two real parameters are necessary to describe each direction). With a large  $D$ , it is possible to perform a Taylor expansion on (2), yielding

$$\begin{aligned} \Delta_{\text{SWM},ij} &= \vec{a}_{r,i}\vec{u}_r - \vec{a}_{t,j}\vec{u}_t \\ &+ \frac{1}{2D} \left[ \|\mathbf{R}(\delta)\vec{a}_{r,i} - \vec{a}_{t,j}\|_2^2 - (\vec{a}_{r,i}\vec{u}_r - \vec{a}_{t,j}\vec{u}_t)^2 \right] \\ &+ o\left(\frac{(R_t+R_r)^2}{2D}\right), \end{aligned} \quad (3)$$

where  $R_x = \max\|\vec{a}_{x,i}\|$  with  $x = t, r$ . What if only the first few orders of the expansion are considered?

**Plane Wave Model.** Approximating  $\Delta_{\text{SWM},ij}$  by its first order Taylor expansion yields

$$\Delta_{\text{PWM},ij} = \vec{a}_{r,i}\vec{u}_r - \vec{a}_{t,j}\vec{u}_t,$$

and leads to the well-known PWM where spherical wavefronts are approximated by planes. The PWM channel coefficient is then

$$h_{\text{PWM},ij} = \rho e^{j\phi} e^{-j\frac{2\pi}{\lambda}(\vec{a}_{r,i}\vec{u}_r - \vec{a}_{t,j}\vec{u}_t)},$$

and the PWM channel matrix can be expressed as

$$\mathbf{H}_{\text{PWM}} = \sqrt{N_t N_r} \rho e^{j\phi} \mathbf{e}_r(\vec{u}_r) \mathbf{e}_t(\vec{u}_t)^H,$$

where contributions to the phase shift of the transmitter and receiver are gathered in the well-known *steering vectors*

$$\mathbf{e}_x(\vec{u}) \triangleq \frac{1}{\sqrt{N_x}} \begin{pmatrix} e^{-j\frac{2\pi}{\lambda}\vec{a}_{x,1}\vec{u}} \\ \vdots \\ e^{-j\frac{2\pi}{\lambda}\vec{a}_{x,N_x}\vec{u}} \end{pmatrix}, \text{ with } x = t, r.$$

Steering vectors depend only on the direction of propagation and are insensitive to the transmission distance  $D$ . The PWM is thus by construction unable to take into account the curvature of the wavefronts. The PWM channel matrix  $\mathbf{H}_{\text{PWM}}$  is a deterministic function of a set of six parameters denoted  $\boldsymbol{\theta} \triangleq \{(\rho, \phi, \vec{u}_t, \vec{u}_r)\}$ , which makes it less complex than the SWM but also less accurate especially when  $D$  is small, as will be shown in section III.

**Parabolic Wave Model.** The two models presented so far are extreme: the SWM considers spherical wavefronts and the PWM approximates the spheres by planes. An intermediate solution is to approximate spheres by paraboloids by considering the second order of the Taylor expansion derived in (3), yielding

$$\Delta_{\text{ParWM},ij} = \vec{a}_{r,i}\vec{u}_r - \vec{a}_{t,j}\vec{u}_t + \frac{1}{2D} \left[ \|\mathbf{R}(\delta)\vec{a}_{r,i} - \vec{a}_{t,j}\|_2^2 - (\vec{a}_{r,i}\vec{u}_r - \vec{a}_{t,j}\vec{u}_t)^2 \right].$$

This expression comprises the PWM term and a correction whose amplitude is inversely proportional to the distance  $D$ . The ParWM channel coefficient is then

$$h_{\text{ParWM},ij} = \rho e^{j\phi} e^{-j\frac{2\pi}{\lambda} \left( \vec{a}_{r,i}\vec{u}_r - \vec{a}_{t,j}\vec{u}_t + \frac{1}{2D} \left[ \|\mathbf{R}(\delta)\vec{a}_{r,i} - \vec{a}_{t,j}\|_2^2 - (\vec{a}_{r,i}\vec{u}_r - \vec{a}_{t,j}\vec{u}_t)^2 \right] \right)}.$$

$\mathbf{H}_{\text{ParWM}}$  is a deterministic function of a set of eight parameters denoted  $\boldsymbol{\theta} \triangleq \{(\rho, \phi, \vec{u}_t, \vec{u}_r, D, \delta)\}$ . Intuitively it is obvious that the ParWM is more accurate than the PWM but less than the SWM: it will be characterized quantitatively in section III. However having more parameters to estimate makes it more complex than the PWM highlighting an accuracy/complexity trade-off. It has the same number of parameters as the SWM but is more tractable: its simpler expressions ease the interpretations and getting rid of the square root might have an interest for hardware implementation of estimation algorithms. **Single-antenna receiver and multipath channel.** As mentioned previously, the three physical models are valid for any  $N_t, N_r$  in a single path LoS scenario. However, further assuming a single antenna receiver ( $N_r = 1$  which implies  $\vec{a}_{r,1} = \vec{0}$ ) allows to simplify the derivations. In that particular case, the above expressions are also valid for paths that originate from reflections on perfect planes [14]. The single-antenna receiver case is of interest since it corresponds to a cellular network scenario with a multi-antenna base station and multiple single-antenna user terminals [10], [11], [14], it is studied in the remaining of the paper. It allows to derive a general expression of the channel valid for the three models in a multipath scenario ( $p$  paths) as a linear combination of *characteristic vectors*:

$$\mathbf{h}_{\mathcal{M}} = \sqrt{N_t} \sum_{k=1}^p \rho_k e^{j\phi_k} \mathbf{e}_{\mathcal{M}}(\vec{u}_{t,k}, D_k) \quad (4)$$

where  $\vec{u}_{t,k}$  and  $D_k$  are the DoD and distance of the  $k$ -th path,  $\mathcal{M}$  denotes the considered model (PWM, ParWM or SWM), and the characteristic vector  $\mathbf{e}_{\mathcal{M}}(\vec{u}_{t,k}, D_k)$  takes the general form

$$\mathbf{e}_{\mathcal{M}}(\vec{u}_{t,k}, D_k) = \frac{1}{\sqrt{N_t}} \begin{pmatrix} e^{-j\frac{2\pi}{\lambda} \Delta_{\mathcal{M},1k}} \\ \vdots \\ e^{-j\frac{2\pi}{\lambda} \Delta_{\mathcal{M},N_t k}} \end{pmatrix},$$

with

- $\Delta_{\text{PWM},jk} = -\vec{a}_{t,j} \cdot \vec{u}_{t,k}$ ,
- $\Delta_{\text{ParWM},jk} = -\vec{a}_{t,j} \cdot \vec{u}_{t,k} + \frac{1}{2D_k} \left[ \|\vec{a}_{t,j}\|^2 - (\vec{a}_{t,j} \cdot \vec{u}_{t,k})^2 \right]$ ,
- $\Delta_{\text{SWM},jk} = \sqrt{D_k^2 - 2D_k(\vec{a}_{t,j} \cdot \vec{u}_{t,k}) + \|\vec{a}_{t,j}\|_2^2} - D_k$ .

These expression are obtained simply by considering  $N_r = 1$  and  $\vec{a}_{r,1} = \vec{0}$  in the expressions of  $\Delta_{\text{PWM},ij}$ ,  $\Delta_{\text{ParWM},ij}$  and  $\Delta_{\text{SWM},ij}$ . Note that the PWM characteristic vectors depend only upon  $\vec{u}_t$ , they are simply steering vectors. On the other hand, the distance  $D$  has an influence on the ParWM and SWM characteristic vectors, since it determines the curvature of the wavefronts.

### III. VALIDITY DOMAINS

In this section, the goal is to characterize the distance ranges where the different models are describing correctly the channel in the simple LoS case. The channel is assumed to follow the SWM and the aim is to assess the PWM and ParWM accuracies.

**Approaches.** In the literature [9], [13] a phase shift difference of at most  $\frac{\pi}{8}$  with respect to the SWM phase shift  $\frac{2\pi}{\lambda} \Delta_{\text{SWM},jk}$  is used to define the PWM validity. Bounding

$\frac{2\pi}{\lambda} |\Delta_{\text{SWM},jk} - \Delta_{\text{PWM},jk}|$  and  $\frac{2\pi}{\lambda} |\Delta_{\text{SWM},jk} - \Delta_{\text{ParWM},jk}|$  using the fact that  $|\vec{a}_{t,j} \cdot \vec{u}_t| \leq R_t$ , this yields

- $D \geq \frac{8R_t^2}{\lambda}$  for the PWM, this boundary is often called the Fraunhofer distance [9].
- $D \geq \sqrt{\frac{8R_t^3}{\lambda}}$  for the ParWM, this boundary is sometimes called the Fresnel distance [9].

This method has several drawbacks: it considers an arbitrary phase-shift difference of  $\frac{\pi}{8}$ , does not apply to the overall channel matrix (it is based on individual channel coefficients) and is independent of the relative position of the emitter and receiver. To overcome these drawbacks another metric is introduced called relative model approximation error (rMAE):

$$\text{rMAE} = \frac{\|\mathbf{h} - \text{proj}_{\mathcal{M}}(\mathbf{h})\|_2^2}{\|\mathbf{h}\|_2^2},$$

where  $\text{proj}_{\mathcal{M}}(\mathbf{u}) \triangleq \text{argmin}_{\mathbf{x} \in \mathcal{M}} \|\mathbf{u} - \mathbf{x}\|_2$  and  $\mathbf{h}$  refers to the true channel (the SWM being taken as the reference,  $\mathbf{h} = \mathbf{h}_{\text{SWM}}$ ). The rMAE assesses the best approximation of the channel that can be obtained with the considered model.

**Setting.** The objective is to study this new metric in a single path LoS scenario varying the array shape (ULA, square UPA), the number of antennas (64, 256), the emitter-receiver distance (from  $\lambda$  to  $10^5 \lambda$ ) and the considered model. A  $\frac{\lambda}{2}$  antenna spacing and a single-antenna receiver located in front of the transmit array (yielding a DoD orthogonal to the array) are considered. It is to be stressed that the obtained curves are parameterized by the wavelength and thus valid irrespective of the band, even though massive MIMO antenna arrays are more likely to be used at small wavelength (e.g. millimeter waves).

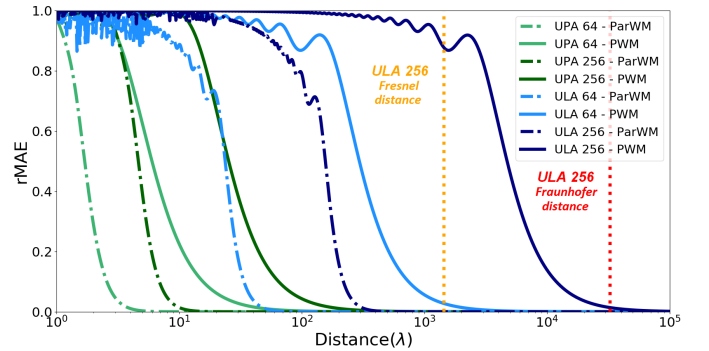


Fig. 1: rMAE for the PWM and ParWM varying  $D$ ,  $N_t$  and the array shape.

**Results.** The figure 1 provides rMAE plots as a function of the normalized distance, expressed on a logarithmic scale, for different configurations. Several comments are in order:

- As expected, at very high distances the rMAE converges to 0 meaning all the models are equivalent and describe the channel correctly. Nevertheless, the convergence occurs at distances much smaller for the ParWM than for the PWM: for instance, with a ULA of 256 antennas, obtaining  $\text{rMAE} < 5\%$  at 30GHz requires  $D > 2.5\text{m}$  for the ParWM and  $D > 170\text{m}$  for the PWM. In such a setting, the PWM is not suitable, whereas the ParWM is sufficiently accurate.

Obviously considering a ULA with less antennas (here 64) reduces the critical distances.

- Another important observation is that even with many antennas, UPAs do not incur large errors: a rMAE of 5% is reached at 1m with 256 antennas. This is simply because for a given number of antennas, UPAs are much smaller than ULAs. Actually,  $R_t$  is proportional to  $N_t$  for an ULA and to  $\sqrt{N_t}$  for an UPA.
- Finally, the yellow (red) vertical line gives the distance boundary for the ParWM (PWM) computed using phase shifts with a ULA of 256 antennas. Beyond this line which corresponds to  $D=15\text{m}$  ( $D=320\text{m}$ ) at 30GHz, the error is as expected negligible.

This study highlights the limits of the PWM at short distances in a novel way, considering the channel matrix globally. On the other hand, the ParWM is shown to be accurate at such short distances, under which users are likely to be present in practical situations. Additionally, it clearly shows that ULAs are more challenging for the PWM than UPAs for which the PWM is accurate from short distances, which is in line with theory.

#### IV. ESTIMATION ALGORITHMS

In the previous section, the intrinsic accuracy of models was assessed. Let us now study how to estimate the channel using these models, based on noisy observations. Indeed, channel state information (CSI) is essential to optimize the capacity of mMIMO systems. Consider a training based estimation strategy in which  $N_s$  noisy linear measurements of the channel are obtained:

$$\mathbf{y} = \mathbf{X}\mathbf{h} + \mathbf{n}, \quad (5)$$

where  $\mathbf{y} \in \mathbb{C}^{N_s}$  is the observation,  $\mathbf{X} \in \mathbb{C}^{N_s \times N_t}$  is the observation matrix and  $\mathbf{n} \in \mathbb{C}^{N_s}$  is the noise vector. Under the additive white Gaussian noise (AWGN) assumption ( $\mathbf{n} \sim \mathcal{CN}(0, \sigma^2 \mathbf{I}_d)$ ), a classical estimation technique is the maximum likelihood (ML), which according to the considered models (4) can be written as

$$\underset{\mathbf{E}, \boldsymbol{\alpha}}{\text{minimize}} \|\mathbf{y} - \mathbf{X}\mathbf{E}\boldsymbol{\alpha}\|_2^2, \quad \hat{\mathbf{h}} \leftarrow \mathbf{E}\boldsymbol{\alpha}$$

where  $\mathbf{E} \triangleq (\mathbf{e}_{\mathcal{M}}(\vec{u}_{t,1}, D_1), \dots, \mathbf{e}_{\mathcal{M}}(\vec{u}_{t,p}, D_p))$ ,  $\boldsymbol{\alpha} \triangleq \sqrt{N_t}(\rho_1 e^{j\phi_1}, \dots, \rho_p e^{j\phi_p})^T$  and  $\hat{\mathbf{h}}$  is the channel estimate. Note that given  $\mathbf{E}$ , the optimal vector  $\boldsymbol{\alpha}$  can be obtained as the solution of a least squares problem as  $\boldsymbol{\alpha}_{\text{opt}} = (\mathbf{E}^H \mathbf{X}^H \mathbf{X} \mathbf{E})^{-1} \mathbf{E}^H \mathbf{X}^H \mathbf{y}$ , so that in the end channel estimation amounts to find an optimal  $\mathbf{E}$ , i.e. an optimal set of  $p$  characteristic vectors  $\{\mathbf{e}_{\mathcal{M}}(\vec{u}_{t,1}, D_1), \dots, \mathbf{e}_{\mathcal{M}}(\vec{u}_{t,p}, D_p)\}$ .

**Greedy strategy for PWM.** Looking for the  $p$  vectors jointly yields a very complex optimization problem. Instead, greedy strategies have been proposed in the PWM case which consist in building a dictionary of characteristic (steering) vectors corresponding to  $N_{\vec{u}_t}$  DoDs and applying a sparse recovery algorithm such as orthogonal matching pursuit (OMP) [17], [18]. This amounts to estimate the paths one by one, i.e. building the matrix  $\mathbf{E}$  column by column. Denoting  $\mathbf{E}^{(k)} \triangleq (\mathbf{e}_{\text{PWM}}(\vec{u}_{t,1}, D_1), \dots, \mathbf{e}_{\text{PWM}}(\vec{u}_{t,k}, D_k))$  the state of the matrix  $\mathbf{E}$  at the  $k$ -th iteration, the optimal vector  $\boldsymbol{\alpha}^{(k)} \leftarrow (\mathbf{E}^{(k)H} \mathbf{X}^H \mathbf{X} \mathbf{E}^{(k)})^{-1} \mathbf{E}^{(k)H} \mathbf{X}^H \mathbf{y}$  is computed so that

a residual  $\mathbf{r}^{(k+1)} \leftarrow \mathbf{y} - \mathbf{X} \mathbf{E}^{(k)} \boldsymbol{\alpha}^{(k)}$  is used at the next iteration. The actual choice of the  $k$ -th column of  $\mathbf{E}$  is done by finding

$$\vec{u}_{t,k} \leftarrow \underset{\vec{u}_t}{\text{argmax}} \frac{|\mathbf{r}^{(k)H} \mathbf{X} \mathbf{e}_{\text{PWM}}(\vec{u}_t)|}{\|\mathbf{X} \mathbf{e}_{\text{PWM}}(\vec{u}_t)\|_2}, \quad (S_{\text{PWM}})$$

among the  $N_{\vec{u}_t}$  test directions. The complexity of this strategy is dominated by the computation of  $N_{\vec{u}_t}$  inner products in  $\mathbb{C}^{N_t}$ .

**Joint strategy for SWM and ParWM.** One possible, although naive way to handle the SWM and ParWM is to directly adapt the previous strategy except that the choice of the  $k$ -th column of  $\mathbf{E}$  is done by finding

$$\vec{u}_{t,k}, D_k \leftarrow \underset{\vec{u}_t, D}{\text{argmax}} \frac{|\mathbf{r}^{(k)H} \mathbf{X} \mathbf{e}_{\mathcal{M}}(\vec{u}_t, D)|}{\|\mathbf{X} \mathbf{e}_{\mathcal{M}}(\vec{u}_t, D)\|_2}, \quad (S_{\text{joint}})$$

where  $\mathcal{M}$  stands for ParWM or SWM. Testing jointly  $N_{\vec{u}_t}$  directions and  $N_D$  distances, solving this optimization problem amounts to test  $N_{\vec{u}_t} N_D$  vectors  $\mathbf{e}_{\mathcal{M}}(\vec{u}_t, D)$ . This yields a complexity dominated by the computation of  $N_{\vec{u}_t} N_D$  inner products in  $\mathbb{C}^{N_t}$ .

**Sequential strategy for SWM and ParWM.** In order to reduce the computational cost, it is possible to depart more from the classical OMP by estimating the direction and distance sequentially, assuming an infinite distance during the direction determination (which amounts to consider the PWM), yielding

$$\begin{aligned} \vec{u}_{t,k} &\leftarrow \underset{\vec{u}_t}{\text{argmax}} \frac{|\mathbf{r}^{(k)H} \mathbf{X} \mathbf{e}_{\text{PWM}}(\vec{u}_t)|}{\|\mathbf{X} \mathbf{e}_{\text{PWM}}(\vec{u}_t)\|_2}, \\ D_k &\leftarrow \underset{D}{\text{argmax}} \frac{|\mathbf{r}^{(k)H} \mathbf{X} \mathbf{e}_{\mathcal{M}}(\vec{u}_{t,k}, D)|}{\|\mathbf{X} \mathbf{e}_{\mathcal{M}}(\vec{u}_{t,k}, D)\|_2}. \end{aligned} \quad (S_{\text{seq}})$$

Testing  $N_{\vec{u}_t}$  directions and  $N_D$  distances, solving this optimization problem amounts to test  $N_{\vec{u}_t}$  vectors  $\mathbf{e}_{\text{PWM}}(\vec{u}_t, D)$  and then  $N_D$  vectors  $\mathbf{e}_{\mathcal{M}}(\vec{u}_{t,k}, D)$ . This yields a complexity dominated by the computation of only  $N_{\vec{u}_t} + N_D$  inner products in  $\mathbb{C}^{N_t}$ .

**Preliminary experiment.** Let us compare empirically the three aforementioned strategies in a multi-user MIMO scenario, with realistic channels generated by the QuaDRiGa channel simulator [19]. We consider a micro-cell operating at a frequency of 28 GHz with the 3GPP\_38.901\_UMi\_LOS scenario of QuaDRiGa. We use a base station (BS) equipped with an ULA comprising 256 antennas (separated by half-wavelengths) at a height of 5 meters and one hundred users equipped with a single antenna at a height of 1.5 meters, which are randomly located at an azimuth angle between  $-45^\circ$  and  $45^\circ$  with respect to the BS array broadside and at a distance between 10 and 20 meters. The idea is to mimic a base station on the frontage of a building communicating with users in the adjacent street. The SNR is set to 5 dB and it is assumed that the users send orthogonal pilots to the BS. This fits the framework of (5) with  $\mathbf{X} = \mathbf{I}_d$  for each user (after correlation at the BS).  $N_{\vec{u}_t} = 300$  test directions uniformly sampling  $[0, \pi]$ , and  $N_D = 30$  test distances logarithmically distributed between 1 and 500 meters are tested.

**Results.** The experiment results for a varying number of estimated paths  $p$  are shown in figure 2, with the average estimation time of each method. The metric used to assess

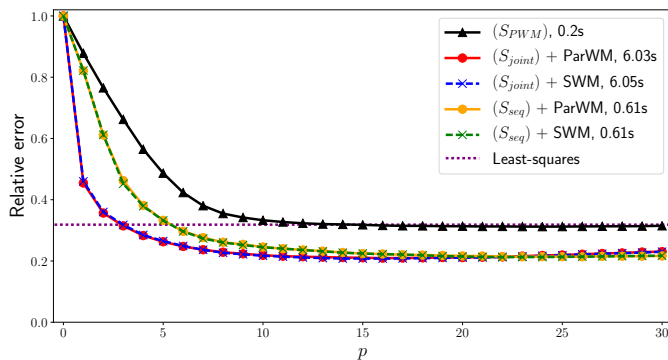


Fig. 2: Comparison of the estimation algorithms.

the estimation strategies is the relative error  $\frac{\|\mathbf{h} - \hat{\mathbf{h}}\|_2^2}{\|\mathbf{h}\|_2^2}$  averaged over the 100 users, and the classical least-squares estimator is also shown as a reference. Several comments are in order:

- First of all, as expected, the strategies  $(S_{\text{joint}})$  and  $(S_{\text{seq}})$  are much better than  $(S_{\text{PWM}})$ . This is because they take into account the wavefronts curvature. They are also better than the least-squares (this is especially true at low SNR), because of the low number of parameters to estimate in the physical models, compared to the number of antennas.
- Moreover,  $(S_{\text{seq}})$  is almost as good as  $(S_{\text{joint}})$  (as soon as  $p > 10$ ), which shows its interesting potential. It is indeed much more computationally efficient than  $(S_{\text{joint}})$  (around ten times faster in the tested configuration on a laptop with an Intel(R) Core(TM) i7-3740QM CPU @ 2.70 GHz).
- Finally, ParWM and SWM are equivalent in the considered setting, despite ParWM being simpler (it does not involve square roots). This is interesting for a hardware implementation in which complex operations are preferably avoided.

## V. CONCLUSIONS AND PERSPECTIVES

In this paper three physical channel models applicable to massive MIMO and any type of antenna array have been studied in an unified way: the well-known PWM, the SWM and the novel ParWM which yields an interesting accuracy-complexity trade-off. The models accuracies have been assessed, underlining the PWM limitations in particular when large ULAs are considered, which is plausible in practical massive MIMO scenarios. Two estimation algorithms taking the wavefronts curvature (SWM or ParWM) into account have been proposed, compared to the classical PWM approach and shown to be more accurate at short distance. In particular, a computationally efficient strategy in which the DoD and distance are estimated sequentially has been proposed, showing promising results.

In the future, a more extensive experimental evaluation of the proposed algorithms should be undertaken (varying the distance and the SNR). Moreover, generalizing the proposed channel estimation methods to multi-antenna receivers and considering other scenarios would be of great interest. For example, one could envision using the SWM/ParWM in a downlink channel estimation scenario, in order to reduce the pilot sequences duration, thanks to the a priori information embedded in the models. Another possibility, in the framework of hybrid systems based on beam sweeping, is to design

optimized beams based on the SWM/ParWM characteristic vectors instead of on steering vectors for users close to the BS.

## REFERENCES

- [1] E. Björnson, J. Hoydis, L. Sanguinetti *et al.*, “Massive MIMO networks: Spectral, energy, and hardware efficiency,” *Foundations and Trends in Signal Processing*, vol. 11, no. 3-4, pp. 154–655, 2017.
- [2] E. G. Larsson, O. Edfors, F. Tufvesson, and T. L. Marzetta, “Massive MIMO for next generation wireless systems,” *IEEE Communications Magazine*, vol. 52, no. 2, pp. 186–195, 2014.
- [3] L. Lu, G. Y. Li, A. L. Swindlehurst, A. Ashikhmin, and R. Zhang, “An overview of massive MIMO: Benefits and challenges,” *IEEE Journal of Selected Topics in Signal Processing*, vol. 8, no. 5, pp. 742–758, 2014.
- [4] F. Rusek, D. Persson, B. K. Lau, E. G. Larsson, T. L. Marzetta, O. Edfors, and F. Tufvesson, “Scaling up MIMO: Opportunities and challenges with very large arrays,” *IEEE Signal Processing Magazine*, vol. 30, no. 1, pp. 40–60, 2013.
- [5] A. L. Swindlehurst, E. Ayanoglu, P. Heydari, and F. Capolino, “Millimeter-wave massive MIMO: the next wireless revolution?” *IEEE Communications Magazine*, vol. 52, no. 9, pp. 56–62, 2014.
- [6] T. S. Rappaport, S. Sun, R. Mayzus, H. Zhao, Y. Azar, K. Wang, G. N. Wong, J. K. Schulz, M. Samimi, and F. Gutierrez, “Millimeter wave mobile communications for 5G cellular: It will work!” *IEEE Access*, vol. 1, pp. 335–349, 2013.
- [7] E. Telatar, “Capacity of multi-antenna Gaussian channels,” *European Trans. on Telecommunications*, vol. 10, no. 6, pp. 585–595, 1999.
- [8] L. Le Magoarou and S. Paquelet, “Parametric channel estimation for massive MIMO,” in *IEEE Statistical Signal Processing Workshop (SSP)*, 2018.
- [9] K. T. Selvan and R. Janaswamy, “Fraunhofer and fresnel distances: Unified derivation for aperture antennas,” *IEEE Antennas and Propagation Magazine*, vol. 59, no. 4, pp. 12–15, 2017.
- [10] X. Cheng and Y. He, “Geometrical model for massive MIMO systems,” in *2017 IEEE 85th Vehicular Technology Conference (VTC Spring)*, 2017, pp. 1–6.
- [11] M. M. Tamaddondar and N. Noori, “Plane wave against spherical wave assumption for non-uniform linear massive MIMO array structures in LoS condition,” in *2017 Iranian Conference on Electrical Engineering (ICEE)*, 2017, pp. 1802–1805.
- [12] L. Liu, D. W. Matolak, C. Tao, Y. Li, B. Ai, and H. Chen, “Channel capacity investigation of a linear massive MIMO system using spherical wave model in LoS scenarios,” *Science China Information Sciences*, vol. 59, no. 2, pp. 1–15, 2016.
- [13] L. Liu, D. W. Matolak, C. Tao, Y. Lu, and H. Chen, “Far region boundary definition of linear massive MIMO antenna arrays,” in *2015 IEEE 82nd Vehicular Technology Conference (VTC2015-Fall)*, 2015, pp. 1–6.
- [14] Z. Zhou, X. Gao, J. Fang, and Z. Chen, “Spherical wave channel and analysis for large linear array in LoS conditions,” in *Globecom Workshops, 2015 IEEE*. IEEE, 2015, pp. 1–6.
- [15] F. Bohagen, P. Orten, and G. E. Oien, “On spherical vs. plane wave modeling of line-of-sight MIMO channels,” *IEEE Transactions on Communications*, vol. 57, no. 3, pp. 841–849, 2009.
- [16] J.-S. Jiang and M. A. Ingram, “Spherical-wave model for short-range MIMO,” *IEEE Transactions on Communications*, vol. 53, no. 9, pp. 1534–1541, 2005.
- [17] S. Mallat and Z. Zhang, “Matching pursuits with time-frequency dictionaries,” *Signal Processing, IEEE Transactions on*, vol. 41, no. 12, pp. 3397–3415, Dec 1993.
- [18] W. U. Bajwa, J. Haupt, A. M. Sayeed, and R. Nowak, “Compressed channel sensing: A new approach to estimating sparse multipath channels,” *Proceedings of the IEEE*, vol. 98, no. 6, pp. 1058–1076, June 2010.
- [19] S. Jaekel, L. Raschkowski, K. Börner, and L. Thiele, “Quadriga: A 3-d multi-cell channel model with time evolution for enabling virtual field trials,” *IEEE Transactions on Antennas and Propagation*, vol. 62, no. 6, pp. 3242–3256, 2014.